Frank J. Pipitone
Naval Research Laboratory
Artificial Intelligence Center
Code 7510
Washington, DC 20375

Thomas G. Marshall
Rutgers University
Electrical Engineering Department
Piscataway, NJ 08854

A Wide-field Scanning Triangulation Rangefinder for Machine Vision

Abstract

This paper describes the design, construction, and measured performance of an experimental scanning laser rangefinder. The instrument uses active triangulation and employs an optical bandpass filter to minimize the effects of ambient illumination. Its use of a single photodetecting element, a photomultiplier, is a unique feature among scanning triangulation rangefinders. A novel scanning configuration based on spherical coordinates is employed, resulting in an extremely large field of view. Nearly 75% of the surrounding solid angle is accessible. Reasonably high speed and accuracy are obtained. The typical error in range at a range of 50 in. is .12 in. The typical error in either of the two angular coordinates is .03°. The maximum instantaneous rate of acquisition of range samples is 500 Hz. Much higher speed and accuracy appear achievable with various modifications and improvements. This type of rangefinder appears most useful in automatic surveillance and robot navigation applications, because of its large field of view.

1. Introduction

In recent years it has been recognized that range data are valuable in machine vision applications in which three-dimensional shape is of primary interest (Shirai and Suwa 1971; Rocker and Kiessling 1975; Lewis and Johnston 1977; Yakimovsky and Cunningham 1978; Altschuler, Altschuler, and Taboada 1979; Duda, Nitzan, and Barett 1979; Pipitone 1982). Among such applications are the navigation of an autonomous robotic vehicle for surveillance or for extraterrestrial exploration and the recognition of intruders in surveillance applications. Another application is automatic assembly, where the identities and positions of known objects must be determined. Still another is the automatic inspection of rigid manufactured objects. Military applications include missile guidance by topographic features and automatic identification and tracking of flying targets.

Most existing optical scanning rangefinders fall into two categories; time-of-flight systems and triangulation systems. Most time-of-flight systems consist of a laser, amplitude-modulated with a sinusoid or a periodic pulse waveform, and a fast photodetector (usually a photomultiplier) directed at the spot made by the beam on an object (Lewis and Johnston 1977; Nitzan, Brain, and Duda 1977; SPIE 1978). A measurement is made of the phase of the detected waveform relative to that of the modulating waveform. This phase is a linear function of round-trip time and thus of range. The viewing direction of such a system can be deflected along two angular scanning coordinates by a gimbaled mirror. The chief disadvantage of such systems is severe speed and accuracy trade-off. For example (Nitzan, Brain, and Duda 1977), one sophisticated system requires approximately 0.3 s on the average to obtain an accuracy of 1 cm in a typical indoor scene.

Triangulation rangefinders all use the principles illustrated in Fig. 1 (Shirai and Suwa 1971; Will and Pennington 1971; Agin 1973; Popplestone et al. 1975; Rocker and Kiessling 1975; Nevatia 1976; Yakimovsky and Cunningham 1978; Altschuler, Altschuler, and Taboada 1979; Pipitone 1979; 1981; Boissonnat

Frank J. Pipitone was formerly with Rutgers University.

The International Journal of Robotics Research
Vol. 2, No. 1, Spring 1983
0278-3649/83/010039-11 $05.00/0

Fig. 1. The triangulation ranging principle.

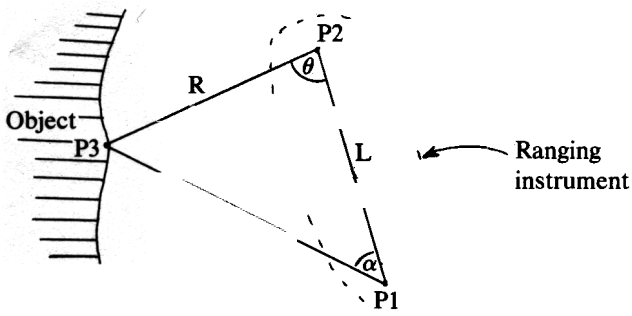

and Germain 1981). A point P3 in the scene is "observed" from both points P1 and P2 in the ranging instrument. Then the angles α and θ between the respective lines of sight and the line P1P2 are measured. From the law of sines, we can then easily compute the range R using the range formula

$$R = \frac{L \sin(\alpha)}{\sin(\theta + \alpha)} \quad (1)$$

Then the ranging system must somehow reorient itself so that a new object, point P3, is "observed." Thus a second range measurement is made, and so on.

The range error formula

$$\Delta R \approx \frac{R^2}{L \sin(\theta)} (\Delta\alpha + \Delta\theta) \quad (2)$$

gives the approximate absolute error ΔR in the range for a triangulation rangefinder. $\Delta\alpha$ and $\Delta\theta$ are the absolute values of the errors in α and θ respectively, in radians. This asymptotic approximation was obtained by differentiating the range formula (Eq. 1) with respect to α and θ and noting its behavior when $R \gg L$.

The basic triangulation geometry described above suggests different classes of instruments. There are many means of "observing" P3 from P1 or P2. We can use a directional detector at both points to obtain one class of instruments. Among such detectors are TV cameras, linear solid-state imaging arrays with lens systems, and single photodetectors with directional optics such as a lens and pinhole.

A second class can be obtained by using a narrowly directed source of light at either P1 or P2 to "observe" P3, with a directional detector at the remaining point. The author's system is of this type. Such a source might project a pattern of lines or spots on the scene instead of a single spot (Shirai and Suwa 1971; Will and Pennington 1971; Agin 1973; Popplestone et al. 1975; Rocker and Kiessling 1975; Altschuler, Altschuler, and Taboada 1979). However, only one point P3 on this pattern is involved in an individual range measurement, and so the geometry of Fig. 1 still applies.

2. The Geometric Basis for Wide-Field Scanning

Figure 2 illustrates a particular way of moving the elements of Fig. 1 to realize a very-wide-field scanning rangefinder. Here the line P1P2 is oriented vertically and is of fixed length L. P1 and P2 are fixed in space, and the part of the instrument containing the directional detector and the laser scan mirror rotates about the line P1P2. The directional detector at P2 (see Section 3 for a particular design) scans within the same plane as does the laser beam, emanating from P1. The angle θ is measured between the line of sight P1P3 and the vertical P1P2, as shown, and is the polar angle (latitude) of a spherical coordinate system centered at P2. The angle ϕ is the azimuthal angle (longitude) of the spherical coordinate system and is the angular position of the subsystem that rotates about the line P1P2. These two angles specify the direction in which the rangefinder operates and correspond to the vertical and horizontal indices of the resulting range picture, R being the pixel value, represented by brightness or pseudocolor in a CRT display.

During operation, the angle α varies rapidly via the rotating, possibly multifaceted mirror at P1 until the beam strikes the point P3 at which the line of sight of the detector at P2 intersects an object surface. Then θ and α can be measured and (Eq. 1) employed to calculate the range R. θ varies uniformly at a slower rate than α and represents the vertical (polar-angle) coordinate of the range picture. α undergoes a complete sweep of the scene, result-

Fig. 2. Wide-field triangulation configuration.

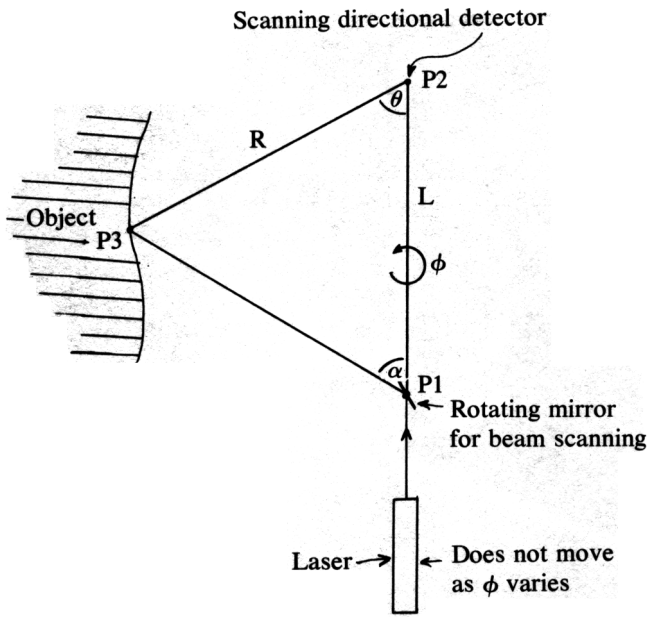

ing in the acquisition of one range datum each time θ varies by some small angle representing the vertical angular separation between range pixels, roughly ½° in this system. After a certain interval in θ has been covered, completing one vertical scan line of measurements (90° in this system), ϕ is incremented by a small angle (½° in this system). Then another vertical scan line is taken at this new azimuthal angle value. The process can be repeated for a full 360° interval in ϕ.

The geometry described above allows a very large field of view. For example, assuming a vertical scan interval of $45° \leq \theta \leq 135°$, the solid angle covered by the instrument is

$$\Omega = \int_{135°}^{45°} 2\pi \sin\theta \, d\theta = 2\sqrt{2}\pi \text{ sr} = 0.71 \times 4\pi \text{ sr}, \quad (3)$$

or 71% of the entire surrounding region. Only the two conical "polar" regions above and below are inaccessible. Note that for a larger interval in θ an even larger field of view is achieved, although accuracy decreases as θ approaches 0° or 180° (see Eq. 2).

It should be pointed out that an alternate version of this system is possible. There are many ways of implementing the scanning directional detector called for at P2 (Pipitone 1982). Suppose we have one that can scan much more rapidly than the rotating mirror at P1 can scan the laser beam. Then we can reverse their roles, using the fast-scanning directional detector at P1 and the slower laser scanner at P2. Such a system appears feasible with no reduction in laser scanning rate and hence would have a line rate equal to the pixel rate of the present system. The alternate version was not implemented because of the time and cost of developing the required detector (Pipitone 1982, p. 33).

3. Overall Architecture and Scanning Subsystems

3. Overall System Architecture

The architecture of the entire system is outlined in Fig. 3, and a photograph of the ranging hardware is shown in Fig. 4. The opto-mechanical scanning hardware is controlled by an interface and control circuit board, seen at the left in Fig. 4. A Digital Equipment Corporation (DEC) LSI-11 computer communicates with this circuit board via a DRV-11 parallel input/output (I/O) port. The main purpose of this communication is the transfer of raw data from the ranging instrument to the LSI-11. The operator controls the system from a printing terminal and uses a color-graphics system as a peripheral to display pseudo-color-coded range pictures.

The detector and laser scanners, described below, are rigidly mounted on a 4-in. diameter aluminum tube as shown in Fig. 4. The distance L separating them is approximately 22 in. Note the vertical slot at the bottom of the tube through which the laser beam emerges from the rotating mirror at P1. A hollow ½-in. diameter steel shaft rigidly attached to the bottom of the tube and mounted in aluminum bushings allows the ϕ rotation and permits the laser beam to pass along the ϕ axis to P1. A stepping motor and gear train mounted below allow ϕ to step by ½° under computer control, moving the entire tube assembly.

Fig. 3. Overall system architecture.

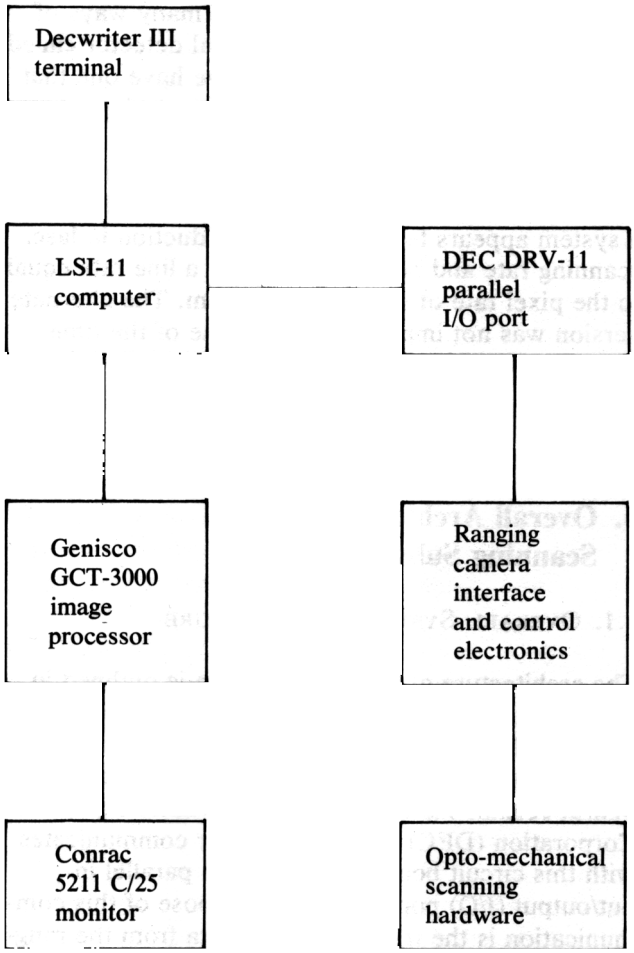

Fig. 4. Rangefinder hardware.

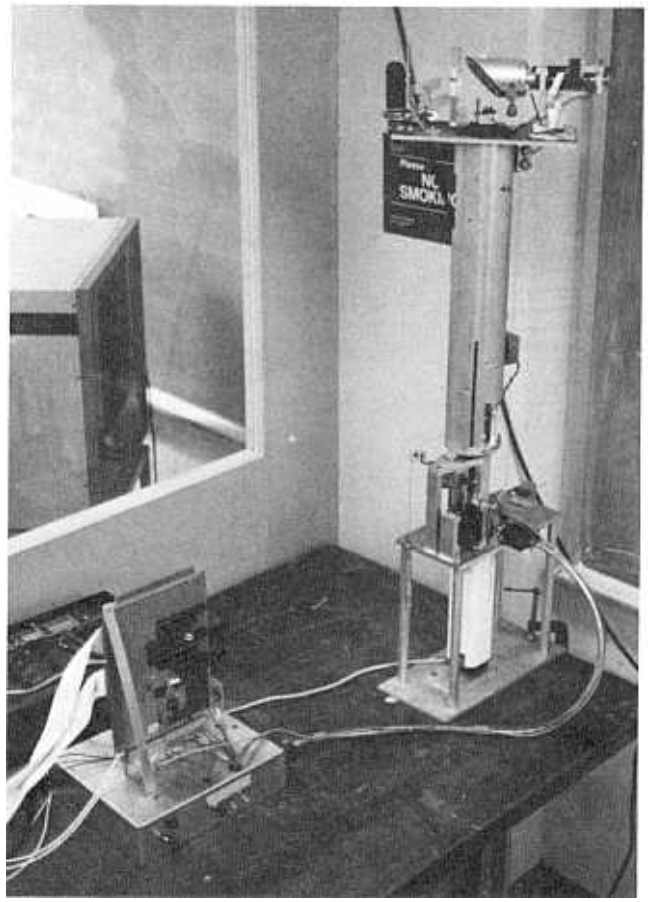

3.2. Scanning Directional Detector

We will begin the detailed description of the instrument with the scanning directional detector centered at point P2 in Fig. 2. This system is shown in a photograph (Fig. 5) and a drawing (Fig. 6). An RCA 4840 photomultiplier is the single photodetecting element in the system, a unique feature; all other known scanning rangefinders use solid-state imaging arrays or vidicons. Mounted on the window of the photomultiplier is a dichroic optical bandpass filter to admit 632.8 nm light from the HeNe laser while suppressing ambient illumination. Now let us assume for simplicity that the slit shown in Fig. 6 at the focal point of the lens is only a pinhole. Then, if the mirror were absent, the photomultiplier would receive light from any illumination source on a narrow "line of sight," more accurately, a steep cone, to the right. The mirror, mounted at 45° to this line of sight and able to rotate about it, deflects the line of sight by 90° at all times, and as it rotates, the resulting line of sight, emerging from P2 at an angle θ with P1P2, sweeps through the same plane as does the laser beam, though at a much slower rate. Thus if the line of sight intersects an object surface point P3, the laser beam will pass through P3 during its scan, resulting in a detection unless it is obstructed by some object.

Now let us abandon the simplifying assumption that the slit is a pinhole. It is then apparent that the

Fig. 5. Scanning directional detector.

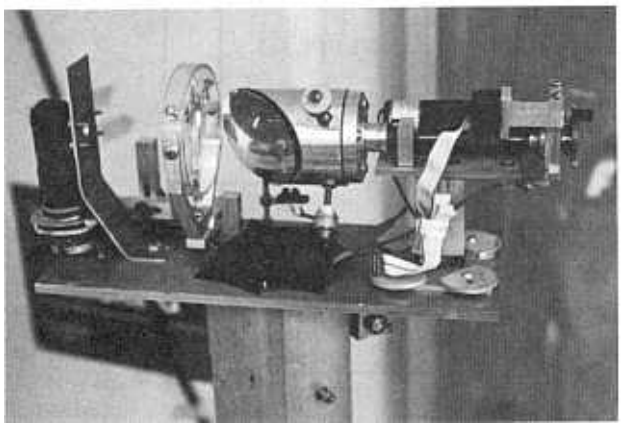

Fig. 6. Simplified drawing of scanning directional detector.

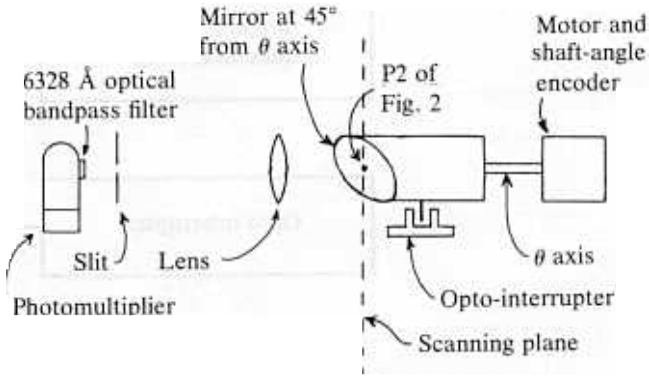

"line of sight" is actually a thin wedge. For $\theta = 90°$, this wedge is perpendicular to the scanning plane as it emanates from P2. Since the laser spot is never outside the scanning plane, detection does occur on a "line of sight" determined by the intersection of the wedge and the plane of the laser beam. The slit is used instead of a pinhole to avoid the difficult alignment that would otherwise be required to make the scanning plane of the detector coincide with that of the laser scanner. As θ varies from 90°, the wedge of sight rotates about its own axis, becoming less nearly perpendicular to the scanning plane, and so the intersection of the scanning plane with the wedge of finite thickness yields a "line of sight" that has increasing angular size (acceptance angle) in θ. In particular, if $\theta = 45°$ or 135°, the extreme values used in this system, the wedge will be rotated about its own axis at 45° with respect to the scanning plane, and the acceptance angle will be greater than that for $\theta = 90°$ by a factor of $\sqrt{2}$, a tolerable increase. A typical acceptance angle in this system is ½°, depending on the adjustment of the slit width. Measurement of the shaft angle θ of the scanning directional detector mirror during a range measurement is accomplished with a Hewlett-Packard HEDS-5000-a03 quadrature shaft-angle encoder. It can resolve $^1/_{2000}$ revolution, and a 12/64 gear pair increases the θ resolution to

$$RES_\theta = \frac{1}{2000} \times \frac{12}{64} \times 360° = 0.03°. \quad (4)$$

Special counter circuitry keeps track of θ. A reference angle is provided by the opto-interrupter shown in Figs. 5 and 6, which sets a flag called θREFFLAG when broken, as illustrated in Fig. 7. A dc gearmotor drives the detector mirror at a rate controlled by a phase-locked loop, as will be described later. A special shaft-angle encoder, comprised of a 48-tooth gear and a copper brush, is used in this phase-locked loop, providing 48 pulses per revolution in θ.

The scanning directional detector and laser scanner run synchronously with a single system clock on the interface and control circuit board. This clock runs at nominally 16.38 MHz and drives a 19-bit binary counter to provide clock rates of 16.38 MHz ÷ 2^n. Only the rates 250 Hz and 31.25 Hz for laser and detector scanning respectively, corresponding to $n = 16$ and $n = 19$, are used. The scanning directional detector's motor is phase-locked to the 31.25-Hz clock by driving the motor with the amplified exclusive-or of the 31.25-Hz clock and the output of the 48-pulse-per-revolution shaft-angle encoder mentioned earlier. This causes θ to vary approximately uniformly at a rate

$$\dot{\theta} = 31.25 \text{ Hz} \div 48 = 0.651 \text{ r/s}. \quad (5)$$

3.3. The Laser Scanner

The Globe-TRW 41A100-13 dc motor, used to drive the scanning directional detector's mirror at point P1 of Fig. 2, is controlled in a similar way to the

Fig. 7. Simplified diagram of data-acquisition electronics.

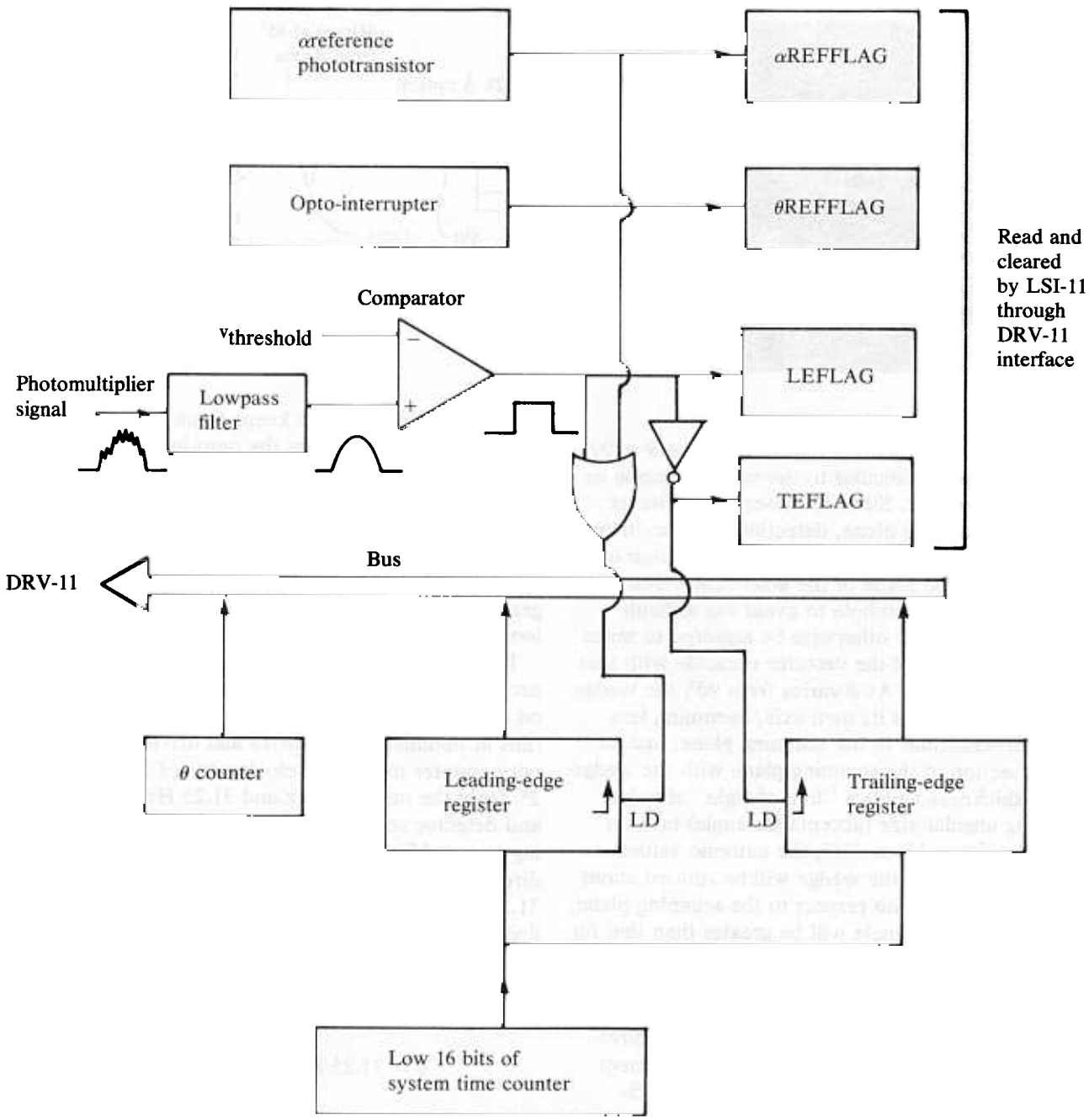

detector scanner. A phototransistor within the cylindrical aluminum housing of the instrument is struck periodically by the laser beam emerging from the mirror, producing 1 pulse per revolution and setting a flag called αREFFLAG, as illustrated in Fig. 7. The motor is driven by the amplified exclusive-or of this signal (after frequency division by two) and the 250-Hz clock, resulting in a motor speed of 500 r/s = 30,000 r/min. The mirror used here is single-faceted, so the laser angle α undergoes 500 sweeps per second, resulting in 500 range measurements per second.

The amount by which θ changes between two consecutive sweeps of α is

$$\delta\theta = 0.651 \text{ r/s} \times 360° \div 500 \text{ sweeps/s} = 0.469°, \quad (6)$$

the average vertical separation between pixels in a range picture from this instrument. The vertical separation between particular adjacent pixels varies somewhat, due in part to jitter in nominally constant $\dot{\theta}$. Even with constant $\dot{\theta}$, the time between detections can vary significantly because α values at detections can vary significantly, for example, at object edges. This then makes a second contribution to nonuniform pixel separation. Since $\dot{\alpha}$ is 1,000 revolutions per second during a laser scan, twice the mirror rotation rate, this effect is kept reasonably small, since the entire (approximately 90°) α scan, during which the detections may occur, occupies only about one-eighth of the laser's rotation period.

3.4. Operation

Overall control of the instrument is exercised by a data-acquisition program, written in FORTRAN, which in turn calls several PDP-11 assembly language subroutines that communicate with the instrument. To operate the instrument, we first "power it up," causing the detector and laser scanners to run continuously in synchronism. Next, we manually rotate the scanning assembly to the desired starting value of ϕ, the azimuthal (horizontal) coordinate. Then we run the acquisition program and enter the desired number of scan lines. The program then alternately steps the ϕ stepping motor by ½° and reads data for a vertical scan line, as described in detail in Section 4.1. After the required number of scan lines is completed, the program halts, having stored the data on a floppy disk after each scan line. A range-computation program later processes these data, as described in Section 4.

4. Generation and Display of Range

4. Data Acquisition

Data for determining α for a range measurement are acquired as follows. The photomultiplier signal is lowpass-filtered to remove high-frequency noise and compared to an adjustable threshold-voltage reference with an analog comparator, as illustrated in Fig. 7. When a detection is made, the resulting photomultiplier pulse gives rise to a square pulse from the comparator. At the leading edge of the comparator pulse, the value of the counter to which the system is synchronized is stored in a register, and a flag called LEFLAG is set. The same is done for the trailing edge of the comparator pulse, using a different register and a flag called TEFLAG. Also, the leading edge of the phototransistor (α reference) pulse receives similar treatment, setting a flag called αREFFLAG and sharing the register loaded at leading edge of the photomultiplier pulse. Thus the system records the real time when the laser beam passes by P3 in Fig. 2 and when it passes through the reference value of α. This information can be used to calculate the α value at which the beam struck P3, since α varies linearly with time.

Now we will describe the details of data acquisition during a line scan, assuming that the data-acquisition program of Section 3.4 has just executed a step of the horizontal coordinate ϕ. Next, it clears the four flags of the interface and control board (see (Fig. 7) and repeatedly polls the opto-interrupter flag θREFFLAG to find the reference value of the vertical-scan coordinate θ. A software delay loop is then executed until θ is somewhat greater than 135° (θ decreases). Then the three flags corresponding to the α reference and to the leading and trailing edges of the photomultiplier pulse are repeatedly polled, and data are read from the corresponding registers to the LSI-11 and stored on a floppy disk.

Fig. 8. Ball and pole.

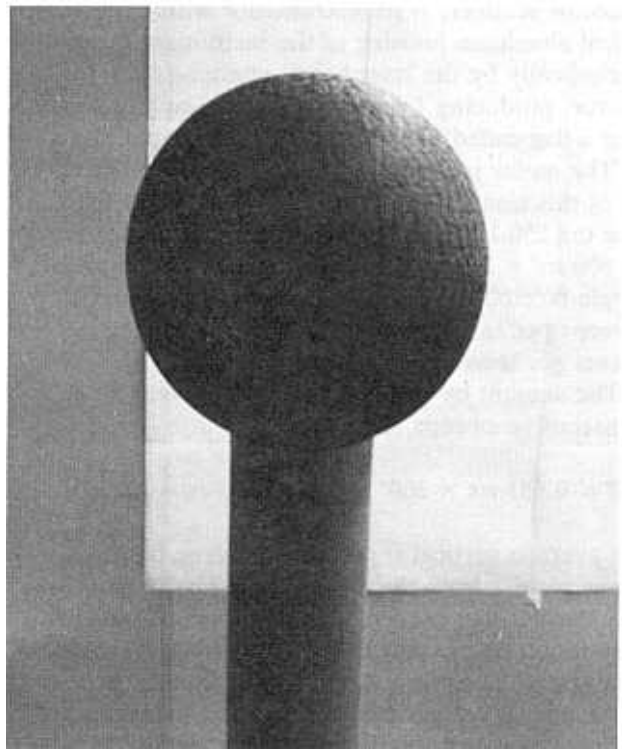

The details of this process for a single pixel are as follows. First, αREFFLAG is polled until it is found to be set, and the α reference time is read from the leading-edge register. Next, LEFLAG is polled. When it is found to be set, the θ value and the leading-edge time are read from the θ counter and the leading-edge register respectively. Then TEFLAG is polled. When it is found to be set, the trailing-edge time is read from the trailing-edge register. αREFFLAG is then polled again to begin the process again for the next pixel.

Data are acquired to span more than 90° in θ. The data stored on disk are a list of ordered quadruples: α reference time, θ value, photomultiplier leading-edge time, and photomultiplier trailing-edge time, one quadruple per pixel. Whenever the photomultiplier pulse is not detected because of a distant, dark, or occluded object point, the three slots for leading edge, trailing edge, and θ are assigned the value 0.

4.2. Range Determination

A second program generates range data from the raw data stored on the floppy disk. This program generates a range value for each quadruple of raw data, using (Eq. 1). The α value used is that corresponding to the time midway between the leading- and trailing-edge times of the photomultiplier pulse. Then for each vertical scan line two arrays of length 192 are generated, one for R and the other for the corresponding θ. The data are "pigeonholed" into these arrays as follows. The interval $45° \leq \theta \leq 135°$ is partitioned into 192 intervals of size 0.46875°, the average pixel separation in θ. Then each measurement (R, θ) is stored in the array elements indexed by the number of the interval in which θ lies. Thus when the range picture is displayed (only the R array is used here), the angle θ will be correctly represented as CRT screen position, independent of jitter in the θ scanner motor.

4.3. Range Display

A third program displays a range picture using a pseudocolor code to make range clearly visible. θ, as approximated by the index of the R array, is the vertical coordinate of the display, and ϕ is the horizontal coordinate. Each pixel is padded to a 3×3 array of identical pixels for convenient scale. Figure 8 shows a 10-in. diameter ball on a 4-in. diameter pole photographed from the vicinity of the range-finder origin P2, roughly 3 ft away. Figures 9 and 10 show a 50-line range picture of the same scene with two different intervals of range mapped into the pseudocolor-code key shown at the upper right in Fig. 9. For example, in Fig. 10, the darkest blue represents a range of 29 in. or less and the deepest red, which appears nearly black, represents a range of 33 in. or greater. Ranges in between are mapped linearly into the color scale shown. The occasional dark spots correspond to those 0.46875° intervals in θ within which no measurement falls because of the nonuniformity of pixel separation discussed earlier. Because a significant part of this nonuniformity is due to jitter in $\dot{\theta}$, which is uncorrelated with the line rate, these spots seem to be randomly located.

Fig. 9. Pseudocolor-coded range picture. Deep red = 43 in.; dark blue = 29 in.

Fig. 10. Pseudocolor-coded range picture. Deep red = 33 in.; dark blue = 29 in.

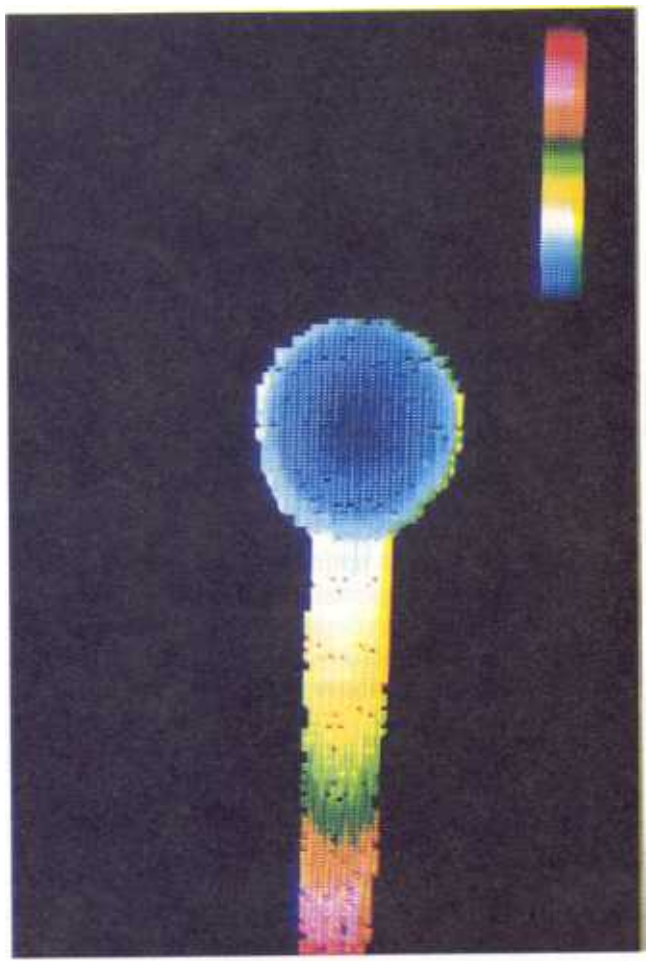

5. Performance

5. Acquisition and Processing Times

Table 1 summarizes the aspects of the performance of the rangefinder discussed in this section. The rate at which range measurements are taken, or the *acquisition rate*, is 500 pixels per second during a vertical scan line. This corresponds to the 500-Hz laser scan mirror-rotation rate. If an octagonal mirror were used instead of the single-faceted one, 4,000 pixels per second would be achieved. More facets would decrease the field in θ, since this field is given by $720° \div \#$ facets $= 90°$ for eight facets. The average acquisition rate obtained over many scan lines is 62 pixels per second. Here a factor of 4 was lost because the θ scanner is only in use during one quarter of its revolution. This could be corrected by adding a "fast-retrace" capability to the control of the θ scanner motor. A factor of 2 was lost because every other θ scan was discarded due to the slow access time of the floppy-disk system. This could of course be remedied by using a storage system with faster access time.

The computation of range data from raw measured data on the disk proceeds at a rate of 20 pixels per second, on the average. This low rate is due to the low speed of the LSI-11 arithmetic operations and

Table 1. Performance Achieved

Parameter	Value	Comments
Acquisition rate during a scan line	500 pixels/s	Single-faced laser scan mirror
Average acquisition rate	62 pixels/s	Factor of 4 lost in 270° inactive θ scan Factor of 2 lost in disk-transfer time
Average-range data-processing rate	20 pixels/s	Limited by speed of LSI-11 arithmetic functions
Maximum range detectable	300 in.	Limited by various noise on photomultiplier signal
Accessible region of the Rθ plane	$R \leq 300$ in. $45° \leq \theta \leq 135°$ $R \geq \frac{22.5(\sin 26.5°)}{\sin (26.5° + \theta)}$	At $\theta = 45°$, $R \geq 10.6$ in. At $\theta = 135°$, $R \geq 31.6$ in.
Accuracy: RMS range error	0.25 in. at 96 in. 0.12 in. at 50 in.	Found by dividing σ of first difference of scan line by $\sqrt{2}$

to the lack of effort in optimizing the program. With a modest amount of special-purpose hardware, the computations could be done in real time, so that finished range data could be generated at the acquisition rates discussed above, while the rangefinder scanned.

5.2. Maximum Range

The maximum range detectable was measured to be approximately 300 in. under ideal conditions; that is, with no ambient lighting and with P3 falling on a sheet of white paper. The signal/noise ratio of the photomultiplier signal was the limiting factor. With the 2.3-in. diameter lens used in the detector, the photomultiplier should theoretically have sufficiently low noise for a maximum range of roughly 10^4 in. However, the unavoidable but small photomultiplier dark noise on which this estimate is based is masked by several much larger contributions from several sources. Among them are the switching power supplies of the laser and photomultiplier, the dc-motor brushes (although EMI suppressors reduce this considerably) and high-frequency ac line noise. These noise contributions could be substantially reduced with a more systematic approach to noise control in the design, including considerations of grounding, shielding, noise suppression, and low-noise-component selection.

5.3. Accessible Region of Space

The region of space accessible to the ranging instrument is a roughly torus-shaped volume coaxial with the ϕ axis of the machine and centered about P2. The region is bounded from above and below by the cones $\theta = 135°$ and $\theta = 45°$ respectively. This 90° vertical field is arbitrary and could easily be increased to include all but a narrow conical region above and below the system. However, a penalty would then be paid in accuracy, which is maximum when $\theta = 90°$ (see Eq. 2). The accessible region is bounded on the inside because of occlusion of the laser beam when $\alpha < 26.5°$. Thus, depending on θ, R can be as small as 10–31 in. This minimum range could be reduced by eliminating some of the mechanical obstructions to the beam in the design. The outer boundary of the region is the sphere whose radius is the maximum range of roughly 300 in., as discussed above.

5.4. Accuracy

The root mean square (RMS) range error measured on a planar surface was approximately 0.25 in. at $R = 96$ in. and 0.12 in. at $R = 50$ in. The accuracy of the instrument depends on the accuracy of measurement of the shaft angles α and θ at which the photomultiplier detections occur, as seen from (Eq.

2), as well as the accuracy of these detections in representing the "centers" of the laser beam and the line of sight. The large acceptance angle (approximately ½°) of the θ scanner was a source of error in the latter. The typical total error in measuring α and θ was approximately 0.03°. The principal ways to reduce range error are therefore to use more accurate shaft-angle encoders, a narrower laser beam, and a scanning-directional detector with a smaller acceptance angle.

6. Conclusion

The feasibility of a scanning triangulation rangefinder having the compact wide-field geometry introduced in Section 2 and using a single photodetecting element has been demonstrated. This arrangement has the unique property that nearly three quarters of the full 4π sr surrounding region can be scanned while achieving moderately high speed and accuracy. Its chief disadvantage is that the three axes of mechanical motion could make it tedious to align and prone to malfunctions. The most appropriate applications envisioned for such a system are automatic surveillance and navigation, due to its wide field. For example, a stationary instrument could be used for the detection and analysis of intrusion in an indoor environment. Its large field would likewise be useful for automatic navigation in an autonomous vehicle.

References

Agin, G. J., and Binford, T. O. (1973) (Aug.). Computer description of curved objects. *Proc. 3rd Int. Joint Conf. Artificial Intell.* Menlo Park, Calif.: SRI International, pp. 629–640.

Altschuler, M., Altschuler, B., and Taboada, J. 1979 (Apr.). Measuring surfaces space-coded by a laser-projected dot matrix. *SPIE Vol. 182, imaging applications for automated inspection and assembly.* Bellingham, Wash.: Society of Photooptical Instrumentation Engineers, pp. 187–191.

Boissonnat, J. D., and Germain, F. 1981 (Aug.). A new approach to the problem of acquiring randomly oriented workpieces from a bin. *Proc. 7th Int. Joint Conf. Artificial Intell.* pp. 796–802.

Duda, R., Nitzan, D., and Barett, P. 1979. Use of range and reflectance data to find planar surface regions. *IEEE Trans. Pattern Anal. Machine Intell.* 1(3):259–271.

Lewis, R. A., and Johnston, A. R. 1977. A scanning laser rangefinder for a robotic vehicle. NASA Tech. Memo. 33-809. Pasadena, Calif.: California Institute of Technology Jet Propulsion Laboratory.

Nevatia, R. 1976. Depth measurement by motion stereo. *Comput. Graphics Image Processing* 5(2):203–214.

Nitzan, D., Brain, A. E., and Duda, R. O. 1977 (Feb.). The measurement and use of registered reflectance and range data in scene analysis. *Proc. IEEE* 65(2):206–220.

Pipitone, F. 1979 (Aug.). A 3-D object recognition system: Ranging camera and algorithm. *SPIE Vol. 205, Image Understanding Systems II.* Bellingham, Wash.: Society of Photooptical Instrumentation Engineers, pp. 61–66.

Pipitone, F. 1982. A ranging camera and algorithms for 3-D object recognition. Ph.D. thesis, Rutgers University.

Popplestone, R., et al. 1975. Forming models of plane-and-cylinder faceted bodies from light stripes. *Proc. 4th Int. Joint Conf. Artificial Intell.* Ann Arbor, Mich.: University Microfilms International, pp. 664–668.

Rocker, F., and Kiessling, A. 1975. Methods for analyzing three dimensional scenes. *Proc. 4th Int. Joint Conf. Artificial Intell.* Ann Arbor, Mich.: University Microfilms International, pp. 669–673.

Shirai, Y., and Suwa, M. 1971 (Sept.). Recognition of polyhedrons with a range finder. *Proc. 2nd Int. Joint Conf. Artificial Intell.* Ann Arbor, Mich.: University Microfilms International, pp. 80–83.

SPIE. 1978 (Mar.). *SPIE Vol. 134, photo and electro-optics in range instrumentation.* Bellingham, Wash.: Society of Photooptical Instrumentation Engineers.

Will, P. M., and Pennington, K. S. 1971 (Sept.). Grid coding: A preprocessing technique for robot and machine vision. *Proc. 2nd Int. Joint Conf. Artificial Intell.* Ann Arbor, Mich.: University Microfilms International, pp. 66–70.

Yakimovsky, Y., and Cunningham, R. 1978. A system for extracting three-dimensional measurements from a pair of TV cameras. *Comput. Graphics Image Processing* 7(2):195–209.